INFECTION AND IMMUNITY, Apr. 2009, p. 1426–1441 Vol. 77, No. 4
0019-9567/09/$08.00+0 doi:10.1128/IAI.00297-08

Host-Pathogen Interactions of *Actinobacillus pleuropneumoniae* with Porcine Lung and Tracheal Epithelial Cells▽†

Eliane Auger,[1] Vincent Deslandes,[1] Mahendrasingh Ramjeet,[1] Irazù Contreras,[2] John H. E. Nash,[3]‡ Josée Harel,[1] Marcelo Gottschalk,[1] Martin Olivier,[2] and Mario Jacques[1]*

Groupe de Recherche sur les Maladies Infectieuses du Porc et Centre de Recherche en Infectiologie Porcine, Faculté de Médecine Vétérinaire, Université de Montréal, Saint-Hyacinthe, Québec J2S 7C6, Canada[1]; Department of Microbiology and Immunology, McGill University, Montréal, Québec H3A 2B4, Canada[2]; and Institute for Biological Sciences, National Research Council of Canada, Ottawa, Ontario, Canada[3]

Received 5 March 2008/Returned for modification 28 April 2008/Accepted 6 January 2009

Host-pathogen interactions are of great importance in understanding the pathogenesis of infectious microorganisms. We developed in vitro models to study the host-pathogen interactions of porcine respiratory tract pathogens using two immortalized epithelial cell lines, namely, the newborn pig trachea (NPTr) and St. Jude porcine lung (SJPL) cell lines. We first studied the interactions of *Actinobacillus pleuropneumoniae*, an important swine pathogen, using these models. Under conditions where cytotoxicity was absent or low, we showed that *A. pleuropneumoniae* adheres to both cell lines, stimulating the induction of NF-κB. The NPTr cells consequently secrete interleukin 8, while the SJPL cells do not, since they are deprived of the NF-κB p65 subunit. Cell death ultimately occurs by necrosis, not apoptosis. The transcriptomic profile of *A. pleuropneumoniae* was determined after contact with the porcine lung epithelial cells by using DNA microarrays. Genes such as *tadB* and *rcpA*, members of a putative adhesin locus, and a gene whose product has high homology to the Hsf autotransporter adhesin of *Haemophilus influenzae* were upregulated, as were the genes *pgaBC*, involved in biofilm biosynthesis, while capsular polysaccharide-associated genes were downregulated. The in vitro models also proved to be efficient with other swine pathogens, such as *Actinobacillus suis*, *Haemophilus parasuis*, and *Pasteurella multocida*. Our results demonstrate that interactions of *A. pleuropneumoniae* with host epithelial cells seem to involve complex cross talk which results in regulation of various bacterial genes, including some coding for putative adhesins. Furthermore, our data demonstrate the potential of these in vitro models in studying the host-pathogen interactions of other porcine respiratory tract pathogens.

Porcine respiratory diseases have heavily impacted the economy of the pig rearing industry worldwide. *Actinobacillus pleuropneumoniae*, an exemplar of these porcine respiratory pathogens, causes porcine pleuropneumonia, a very contagious and often fatal disease characterized by necrotic and hemorrhagic lung lesions, coughing, and severe respiratory distress. Fifteen serotypes of this gram-negative facultative anaerobic bacteria are presently known based on surface polysaccharides (56). The virulence of this pathogen is accomplished with the help of many factors, including exotoxins, endotoxin, capsule polysaccharides, adhesins, and outer membrane proteins, such as iron acquisition systems.

The four pore-forming exotoxins of *A. pleuropneumoniae*, called Apx, are cytolytic and/or hemolytic (20, 51). In fact, the virulence of the different serotypes coincides greatly with the presence of the Apx toxins, particularly ApxI and ApxII. Serotypes 1, 5, 9, and 11 are known to be especially virulent, and all express both ApxI and ApxII (19).

As demonstrated by Jacques et al., lipopolysaccharides (LPS) are the major molecules responsible for adhesion, principally the core oligosaccharide region (45, 48). However, other putative adhesins have also been described, such as type IV fimbriae expressed under specific conditions in different serotypes (63), a 60-kDa collagen-binding protein (14), a 55-kDa outer membrane protein (61), and an autotransporter protein (4).

A close relative of *A. pleuropneumoniae*, *Aggregatibacter (Actinobacillus) actinomycetemcomitans*, was found to be invasive of the human KB cell line and primary gingival cells (17). The invasiveness of this strain has been shown to be related to the colonial morphology, since a switch from a rough to a smooth morphology leads to the loss of its invasive capacity. *Haemophilus parasuis* has also been shown to be invasive of porcine brain microvascular endothelial cells (43, 60). Moreover, *A. actinomycetemcomitans* has been demonstrated to induce cell death by apoptosis of numerous cell types, while the cytolethal distending toxin of *Haemophilus ducreyi* has been shown to induce apoptosis of Jurkat T cells (23, 37). Adherence, invasion, toxin secretion, and other mechanisms involved in the pathogenesis of *Pasteurellaceae* lead to changes in cellular processes, including the induction of nuclear factors and cytokine production. In fact, *A. pleuropneumoniae* stimulates the production of proinflammatory cytokines such as interleukin 1β (IL-1β), IL-8, and tumor necrosis factor alpha (TNF-α), which are detected in alveolar fluid and tissue lesions (56). Likewise, a study by our group demonstrated that the produc-

* Corresponding author. Mailing address: Faculté de Médecine Vétérinaire, Université de Montréal, 3200 Sicotte, St-Hyacinthe, Québec J2S 7C6, Canada. Phone: (450) 773-8521, ext. 8348. Fax: (450) 778-8105. E-mail: mario.jacques@umontreal.ca.

‡ Present address: Office of Biotechnology, Genomics and Population Health, Public Health Agency of Canada, Ottawa, Ontario K1A 0K9, Canada.

† Supplemental material for this article may be found at http://iai.asm.org/.

▽ Published ahead of print on 12 January 2009.

tion of IL-6, TNF-α, IL-1β, MCP-1, and IL-8 by porcine alveolar macrophages is induced by purified serotype 1 *A. pleuropneumoniae* LPS and by heat-killed bacteria (48). IL-8, a neutrophil chemoattractant, is of particular interest, since neutrophil accumulation at the infection site is characteristic of porcine pleuropneumonia (56).

Changes in bacterial gene expression also occur during infection. Studies have been conducted to investigate the gene expression of *A. pleuropneumoniae* under conditions mimicking that of the host. A study by our group used microarray technology to detect changes in gene expression of *A. pleuropneumoniae* serotype 1 grown under iron-restricted conditions (13). In this study, many genes involved in iron acquisition were shown to be upregulated, while genes involved mainly in energy metabolism were downregulated. In vivo studies based on selective capture of transcribed sequences, in vivo expression technology, or signature-tagged mutagenesis (3, 4, 22, 31, 53) have allowed the detection of adhesin and toxin genes and of genes involved in metabolism, stress, regulation, and transport.

Epithelial cells play an important role as the interface between the host mucosal surfaces and the surrounding environment and are the initial site of colonization for most bacterial pathogens. Two porcine respiratory tract epithelial cell lines have been established and described in the literature, namely, the newborn pig trachea (NPTr) (15) and St. Jude porcine lung (SJPL) (52) cell lines. The NPTr cell line was established from a 2-day-old piglet from a pathogen-free herd, while the SJPL cell line was spontaneously established from the lung of a normal 4-week-old female Yorkshire pig (15, 52).

The use of these cell lines has the possibility of generating a great amount of information on the infection mechanism of *A. pleuropneumoniae*, as well as that of other swine bacterial or viral respiratory tract pathogens. Consequently, we developed in vitro models using these cell lines and investigated host-pathogen interactions, including adherence, invasion, and bacterial transcriptomic profile, as well as cell death, nuclear factor expression, and cytokine production by the epithelial cells. This is the first report of models in which immortalized cell lines are used to study interactions of *A. pleuropneumoniae* with respiratory tract epithelial cells of porcine origin.

MATERIALS AND METHODS

Bacterial strains and culture conditions. All strains used in this study are listed in Table 1. All *A. pleuropneumoniae* strains and the *Pasteurella multocida* capsular type A and D strains were grown in brain heart infusion (BHI) broth and/or agar (Gibco, Burlington, VT) supplemented with 15 μg/ml NAD at 37°C in 5% CO_2. The *Actinobacillus suis* strain was grown under the same conditions, with the addition of 25 μg/ml nalidixic acid and 5 μg/ml chloramphenicol. Both *H. parasuis* strains were grown on pleuropneumonia-like organism medium broth and on chocolate agar at 37°C without CO_2.

Cell culture. The NPTr cell line (Instituto Zooprofilattico Sperimental, Brescia, Italy) (15) was grown at 37°C in 5% CO_2 in minimum essential medium (Gibco) supplemented with 10% fetal bovine serum (Gibco) and 1% sodium pyruvate (Gibco). The SJPL cell line (St. Jude Children's Hospital, Memphis, TN) (52) was grown at 37°C in 5% CO_2 in Dulbecco's modified Eagle's medium (DMEM) (Gibco), supplemented with 10% fetal bovine serum, 1% sodium pyruvate, and 1.5% minimal essential medium nonessential amino acids solution (Gibco). Both cell lines were tested by PCR using porcine-specific primers, and amplicons were sequenced to ensure their origin (41).

Cytotoxicity detection assay. The cellular cytotoxicity was measured in the different assays using the lactate dehydrogenase (LDH)-measuring CytoTox 96 nonradioactive cytotoxicity assay (Promega, Madison, WI) as prescribed by the manufacturer. Noninfected cells were used as a negative control, while total lysis of cells by a treatment with 2% Triton X-100 represented the 100%-cytotoxicity positive control. Optical densities at 490 nm were measured with a Power Wave X340 (Biotek Instruments Inc, Winooski, VT) microplate reader and used to calculate the percentage of cytotoxicity.

TABLE 1. Bacterial strains used in the present study

Strain	Serotype	Source or reference
A. pleuropneumoniae S4074	1	K. R. Mittal[a]
A. pleuropneumoniae L20	5b	K. R. Mittal
A. pleuropneumoniae WF83	7	K. R. Mittal
A. pleuropneumoniae FMV91-6514	1 (rough field strain)	32
A. pleuropneumoniae 05-4817	5a (field strain)	K. R. Mittal
A. pleuropneumoniae 05-6501	5b (field strain)	K. R. Mittal
A. pleuropneumoniae 05-3695	7 (field strain)	K. R. Mittal
H. parasuis Nagasaki	5	M. Gottschalk[a]
H. parasuis 29755	5	E. Thacker[b]
A. suis H91-0380	O2/K2	J. MacInnes[c]
P. multocida 88-761	A	K. R. Mittal
P. multocida 1703	D	K. R. Mittal

[a] Faculté de Médecine Vétérinaire, Université de Montréal, St.-Hyacinthe, Canada.
[b] Faculty of Veterinary Medicine, Iowa State University.
[c] Department of Pathobiology, Ontario Veterinary College, University of Guelph, Guelph, Canada.

Apoptosis detection assays. Apoptosis assays were performed using the cell death detection enzyme-linked immunosorbent assay (ELISA) (Roche, Laval, Québec, Canada) and the caspase-3 Western detection kit (Cell Signaling Technology Inc., Beverly, MA) as prescribed by the manufacturers. A bacterial suspension at an optical density at 600 nm (OD_{600}) of 0.6 was added to a confluent monolayer of cells at a multiplicity of infection (MOI) of 10:1 and incubated for 3 h at 37°C in 5% CO_2. Uninfected cells were used as negative controls, and cells treated with 20 μg/ml camptothecin (Sigma) for 4 h at 37°C in 5% CO_2 were used as positive controls. Following the infection, the supernatant and adherent cells were recovered. Plates for the cell death detection ELISA were read at 405 nm in a Power Wave X340 (Biotek Instruments Inc.) microplate reader. For the caspase-3 Western blots, the samples were loaded on a 12% (wt/vol) polyacrylamide gel, migrated at 100 V, and transferred to a nitrocellulose membrane (Bio-Rad, Hercules, CA). The membrane was blocked for 1 h at room temperature in 2% skim milk and then incubated overnight (O/N) at 4°C with polyclonal rabbit antibodies against cleaved caspase-3 and caspase-3. Membranes were washed three times in Tris-buffered saline and incubated with mouse anti-immunoglobulin G antibodies conjugated with horseradish peroxidase for 1 h at ambient temperature and revealed with 3,3′,5,5′-tetramethylbenzidine (Sigma).

Microscopy. Cells were seeded to semiconfluence in four-well LabTekII chamber microscopy slides (Nunc, Naperville, IL) and incubated O/N. One ml of a 2.5×10^6-CFU/ml suspension of *A. pleuropneumoniae* S4074 was added, and slides were then incubated for 2 h at 37°C in 5% CO_2. Following four washes with Dubelcco's phosphate-buffered saline (DPBS) (Gibco), cells were fixed for 10 min in methanol and stained for 30 min with Giemsa stain (Sigma). Four washes with DPBS were performed, and the slides were left to dry. Noninfected cells were also stained as controls. Observation was done at a ×1,000 magnification on a Leica DMR microscope.

Adherence assay. To quantify the adherence of the different strains on both cell lines, 2.5×10^5 epithelial cells were seeded into wells of 24-well tissue culture plates (Sarstedt, Numbrecht, Germany) and incubated O/N. Bacteria from an O/N culture grown at an OD_{600} of 0.6 were resuspended in the adequate cell culture medium to a concentration of 2.5×10^6 CFU/ml. One ml of this suspension was added to each well at an MOI of 10:1, and the plates were incubated from 1 to 3 h. Nonadherent bacteria were removed by washing four times with DPBS. Cell with adherent bacteria were released from the wells by adding 100 μl of 1× trypsin-EDTA (Gibco) and resuspended in 900 μl DPBS buffer. Serial

dilutions were performed, with plating on agar plates to determine the number of bacteria that adhered to the epithelial cells.

Statistical analysis. Data were log transformed prior to analysis. A two-way analysis of variance, with the cell line and the bacterial strain as factors, was used at each time point separately. The level of statistical significance was set at 0.05 throughout. Analyses were carried out using the SAS software program, version 9.1 (SAS, Cary, N C). Contrasts were used to examine differences between pairs of means.

Invasion assay. Epithelial cells (2.5×10^5) were seeded into wells of 24-well tissue culture plates and incubated O/N. One ml of a 2.5×10^7-CFU/ml bacterial suspension was added to the wells (MOI of 100:1). Plates were incubated for 1 to 3 h. Nonadherent bacteria were removed by washing four times with DPBS buffer. One ml of DMEM containing 100 μg/ml of gentamicin was added to each well, followed by a 1-h incubation period at 37°C in 5% CO_2. Killed bacteria were removed by washing twice with DPBS buffer. Cells were then lysed with 100 μl of sterile distilled H_2O, and samples were plated on agar plates and incubated O/N.

Protein profiling of SJPL and NPTr cells in contact with *A. pleuropneumoniae*. Protein profiling of the cells was performed to detect differentially expressed proteins. Two T175 flasks were seeded with a confluent monolayer of cells, and 25 ml of DMEM culture medium with or without 1×10^7 CFU/ml of bacteria grown at an OD_{600} of 0.6 was added to the flasks. Flasks were incubated for 3 h at 37°C in 5% CO_2 and then washed three times with DPBS, and 500 μl of a lysis solution (20 mM morpholinepropanesulfonic acid, 0.5% triton X-100, and protease inhibitors) was added. Cells were removed from the flasks and transferred to microcentrifuge tubes on ice. Sonication at ~180 J was performed using an ultrasonic processor (Cole-Parmer, Vernon Hills, IL) in order to lyse the cells. The samples were then ultracentrifugated at 50,000 rpm for 30 min in a Sorvall RC M100 ultracentrifuge. The supernatant was preserved and analyzed for protein concentration using the Bradford assay (Bio-Rad). Samples were diluted to 2 mg/ml and frozen at −80°C. The samples were then analyzed using the Kinexus antibody microarray, which tracks changes in protein expression of 608 different cell signaling proteins in duplicate, including phosphorylation sites and kinases (Kinex Bioinformatics Inc., Vancouver, British Columbia, Canada). Fifty μg of proteins from both the untreated (control) and treated cells were labeled with the same proprietary fluorescent dye. Each sample was separately applied to opposite sides of the antibody microarray, which contains a dam to prevent mixing of the samples. Following incubation of samples with the Kinex chip, the unbound proteins were washed away and the chips were scanned with a Perkin-Elmer ScanArray Express reader. Image analysis of the TIF files that were produced was performed using the ImaGene 7.0 software program from BioDiscovery (El Segundo, CA). Qualitative and semiquantitative analyses of the expression and phosphorylation states of the cell signaling proteins were performed.

EMSA for detection of NF-κB and AP-1. Cells were infected at an MOI of 1:10 for 30 min, 1 h, or 3 h with *A. pleuropneumoniae* grown at an OD_{600} of 0.6. Uninfected cells were used as a control. Cell stimulation was terminated by the addition of cold phosphate-buffered saline. Six μg of nuclear proteins, extracted as described by Blanchette et al. (9), were incubated for 20 min at room temperature in 1 μl binding buffer (100 mM HEPES [pH 7.9], 40% [vol/vol] glycerol, 10% [wt/vol] Ficoll, 250 mM KCl, 10 mM dithiothreitol, 5 mM EDTA, 250 mM NaCl, and 10 mg/ml bovine serum albumin), and 200 ng/μl poly(dI-dC)–0.02% bromophenol blue with 1 μl of the labeled oligonucleotide containing a consensus sequence of NF-κB/c-Rel homodimeric and heterodimeric complexes (5′A GTTGAGGGGACTTTCCCAGGC-3′; Santa Cruz Biotechnology, Santa Cruz, CA) or of AP-1 complexes (5′CGCTTGATGACTCAGCCGGAA-3′; Santa Cruz Biotechnology) which were previously labeled using T4 polynucleotide kinase and [γ-^{32}P]dATP (GE Healthcare, Piscataway, NJ). After incubation, DNA-protein complexes were resolved by electrophoresis in a 5% (wt/vol) nondenaturing polyacrylamide gel. Subsequently gels were dried and autoradiographed. The nonspecific probes (SP-1 [5′ATTCGATCGGGGCGGGGCGAG-3′] used to confirm the specificity of the DNA/nuclear protein reactions were synthesized in our laboratory. Cold competitor assays were conducted by adding a 100-fold molar excess of homologous unlabeled oligonucleotide for NF-κB or AP-1 and noncompetitor SP-1. For supershift assays, 2 μg of nuclear proteins were incubated with binding buffer, poly(dI-dC), 0.02% bromophenol blue, labeled ologonucleotide, and 4 μg specific antibody (anti-p50 and anti-p65N, both from Santa Cruz Biotechnology) at room temperature for 1 h and complexes resolved on a standard nondenaturing 5% (wt/vol) polyacrylamide gel. For the IRAK inhibition assays, the cells were preincubated for 1 h with 50 μM IRAK 1/4 inhibitor (Calbiochem, Darmstadt, Germany) before addition of the bacteria for an incubation of 3 h. A nuclear protein electrophoretic mobility shift assay (EMSA) was then performed as mentioned above.

Stimulation of cytokine production. Induction assays were performed with both cell lines as described by Ramjeet et al. (48). Briefly, 1 ml culture medium containing 1×10^9 CFU *A. pleuropneumoniae* S4074, heat killed at 60°C for 45 min, was added to wells of 24-well tissue culture plates containing a monolayer of epithelial cells. The plates were incubated from 30 min to 48 h at 37°C in 5% CO_2. The supernatant was then collected and analyzed by ELISA to detect the amounts of IL-1β, TNF-α, IL-6, and IL-8 produced by the stimulated epithelial cells as described by Ramjeet et al. (48). The stimulation tests were also performed using 35 to 3,500 endotoxin units/ml of *A. pleuropneumoniae* serotype 1 S4074 LPS. These LPS concentrations were shown to induce a response in porcine alveolar macrophages (48). As a control, NF-κB inhibition assays were performed where cells were preincubated for 1 h at 37°C in 5% CO_2 with 25 μg/ml caffeic acid phenethyl ester (Sigma) before addition of the bacteria for an additional incubation of 12 h. The supernatant was collected and tested by ELISA for the IL-8 concentration.

RNA extractions for microarray experiments. Monolayers of SJPL cells in T175 flasks were infected for 3 h with 100 μl of an *A. pleuropneumoniae* culture with an OD_{600} of 0.6 (MOI of 10:1). Planktonic bacteria were harvested from the culture supernatant, while adherent bacteria were harvested with the epithelial cells following two washes in phosphate-buffered saline buffer. Ice-cold RNA degradation stop solution (95% ethanol, 5% buffer-saturated phenol) was added to all samples at a 1:10 (vol/vol) ratio, and samples were then frozen at −80°C after a 5-min centrifugation at 4,000 × *g*. The isolation of bacterial RNA was carried out using the Qiagen RNeasy minikit with an in-column DNase treatment, as prescribed by the manufacturer. RNA was further treated with Turbo DNase (Ambion, Tx) as prescribed by the manufacturer.

Transcriptomic microarray experiments. The AppChip1 design was part of the *A. pleuropneumoniae* 5b L20 genome sequencing project led by the team of John Nash (NRC-IBS, Ottawa, Canada). The microarrays used in this study contain PCR amplicons representing all the open reading frames that were identified in the *A. pleuropneumoniae* 5b L20 genome (13, 18). RNA was reverse transcribed to cDNA using Invitrogen Superscript II reverse transcriptase. cDNA was indirectly labeled with monofunctional Cy3 or Cy5 *N*-hydroxysuccinimide ester (Amersham Biosciences, Piscataway, NJ). Samples from planktonic growth or adhesion versus growth in DMEM medium were combined and cohybridized on the microarray. Four hybridizations were conducted for each condition, including a pair of microarrays for which the Cy3 and Cy5 dyes were swapped. Microarray analysis was carried out using the TM4 software suite (The Institute for Genomic Research) and the significant-analysis-of-microarrays algorithm, using a false-discovery-rate value of 0% (50). For the planktonic and adhesion experiments, the Cy5 signal was compared to the Cy3 signal in order to obtain a list of significantly differentially expressed genes. In order to obtain the list of differentially expressed genes between planktonic growth and adhesion, $\log_2$ ratios were compared in TM4, also using the significant-analysis-of-microarrays algorithm. Functional classification was performed using The Institute for Genomic Research's Comprehensive Microbial Resource (47).

Microarray data accession number. Data files have been submitted to the Gene Expression Omnibus (GEO accession number GSE12009).

RESULTS

Effect of bacterial infection on viability of epithelial cells. *A. pleuropneumoniae* expresses potent exotoxins. To ensure cell viability in our experiments, cell death assays were performed at different MOIs (10:1, 100:1, and 1,000:1) and with different incubation periods (0.5 h, 1 h, 2 h, 3 h, and 4 h) with *A. pleuropneumoniae* strain S4074 representing serotype 1. LDH cytotoxicity assays to detect necrosis were first performed. Important cytotoxicity was observed after an incubaction of 4 h (up to 80% at an MOI of 10:1) or with an MOI of 100:1 (up to 40% at 3 h) (data not shown). An MOI of 10:1 and incubation times not surpassing 3 h were chosen for subsequent tests as a result of low cytotoxicity under these conditions (Fig. 1). Since cell death by apoptosis cannot be detected by the LDH test, apoptosis assays were also preformed. An ELISA assay detecting DNA degradation and a Western blot assay detecting caspase-3 activation were carried out and demonstrated that

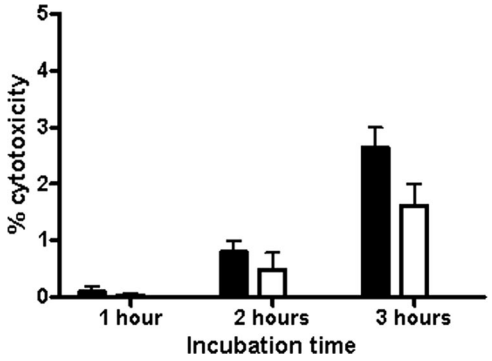

FIG. 1. SJPL (filled bars) and NPTr (empty bars) cells were assessed for cytotoxicity following an infection with *A. pleuropneumoniae* strain S4074 at an MOI of 10:1.

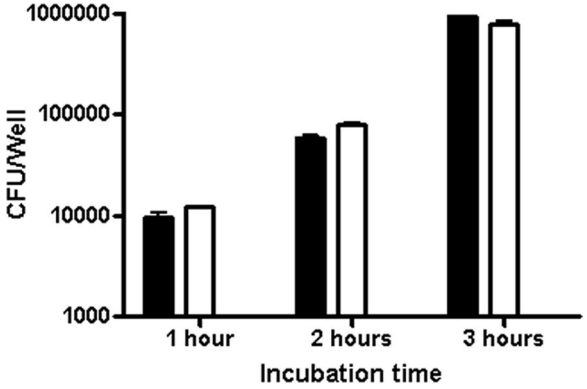

FIG. 3. Adherence of *A. pleuropneumoniae* S4074 to SJPL (filled bars) or NPTr (empty bars) cells from 1 to 3 h.

neither cell line undergoes apoptosis after 3 h of bacterial infection at an MOI of 10:1 (data not shown).

Adherence of *A. pleuropneumoniae*. Standardization of adherence models was performed using both cell lines and the *A. pleuropneumoniae* reference strain S4074. Microscopy assays visually demonstrated the adhesion of the bacteria to the cells (Fig. 2). The increase of adherence over time was well demonstrated in the adherence assay, with an increase of about 1 log every hour (Fig. 3).

Protein profiling of SJPL and NPTr cells incubated with *A. pleuropneumoniae*. Protein profiling of SJPL and NPTr cells incubated with *A. pleuropneumoniae* was performed as a rapid screening method using the Kinexus antibody microarray. Six hundred eight cell signaling proteins, including 250 phospho sites, 240 protein kinases, and 110 cell signaling proteins that regulate cell proliferation, stress,and apoptosis, were represented on the microarray. Only proteins with an *n*-fold change of ± 1 and higher on a $\log_2$ scale were deemed differentially expressed. Twenty proteins were upregulated for the SJPL cells, in contrast to 21 for the NPTr cells, while 25 proteins were downregulated for both the SJPL and NPTr cells (see Tables S1 and S2 in the supplemental material). Among the upregulated proteins, most were implicated in stress response. Mostly proteins implicated in cell growth and proliferation were observed to be downregulated. Among the proteins differentially expressed, IκB kinase α (IKKα), IKKβ, IRAK4, and three different MEKK proteins were detected and directed our focus toward the NF-κB and AP-1 pathways and ultimately to an examination of the production of cytokines by the epithelial cells.

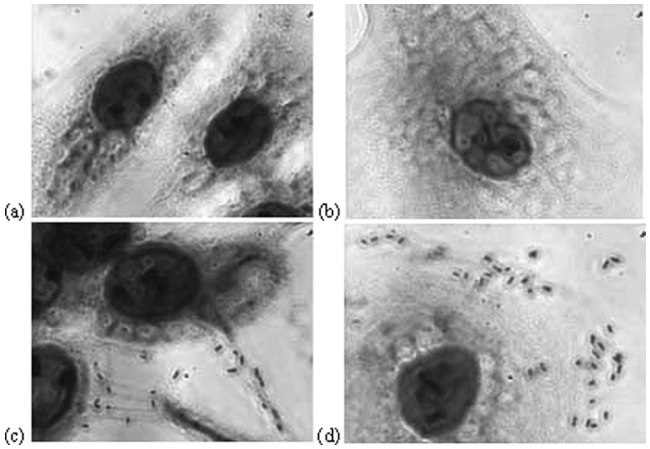

FIG. 2. NPTr (a and c) or SJPL (b and d) cells stained with Giemsa stain in the presence (c and d) or absence (a and b) of *A. pleuropneumoniae* S4074, seen through a Leica DMR microscope at an original magnification of ×1,000.

NF-κB induction and cytokine production. EMSAs detecting the induction of NF-κB and AP-1 were performed on both cell lines following incubation with *A. pleuropneumoniae* S4074, since proteins involved in these pathways were observed to be differentially expressed in our previous experiment. In comparison to the basal level of uninfected cells, a clear induction of NF-κB was noticed for the NPTr cells as soon as at 1 h postinfection which is represented by the appearance of bands of higher density in the upper part of the gel, corresponding to a band shift (Fig. 4A). Only a slight increase in density was observed for the SJPL cells at 3 h postinfection. In order to assess the specificity of the NF-κB induction, a supershift assay using specific antibodies was carried out for the detection of two subunits of NF-κB, p50 and p65. The p50 subunit was found to be induced for the SJPL cells but not the NPTr cells after 3 h of incubation with *A. pleuropneumoniae* S4074, and inversely, the p65 subunit was induced in the NPTr cells only (Fig. 4B). No induction of the AP-1 transcription factor was detected for either cell line in comparison to results for the uninfected cells (data not shown).

To further investigate the bacterium-based induction of the NF-κB transcription factor, we evaluated cytokine production by both cell lines under stimulation conditions. Incubations for up to 48 h of the SJPL and NPTr cells with heat-killed *A. pleuropneumoniae* were then performed to quantify the production of IL-1β, IL-6, IL-8 and TNF-α, proinflammatory cytokines involved in innate immunity, by the epithelial cells. ELISAs performed on the supernatant samples showed that under these conditions, the NPTr cells but not the SJPL cells secrete IL-8. Production of IL-8 by the NPTr cells increased over time to reach 2,500 pg/ml at 48 h (Fig. 5), in comparison to 800 pg/ml with purified LPS. However, no IL-1β, IL-6, or TNF-α was detected in the samples from both cell lines (data not shown). Following inhibition of NF-κB by caffeic acid

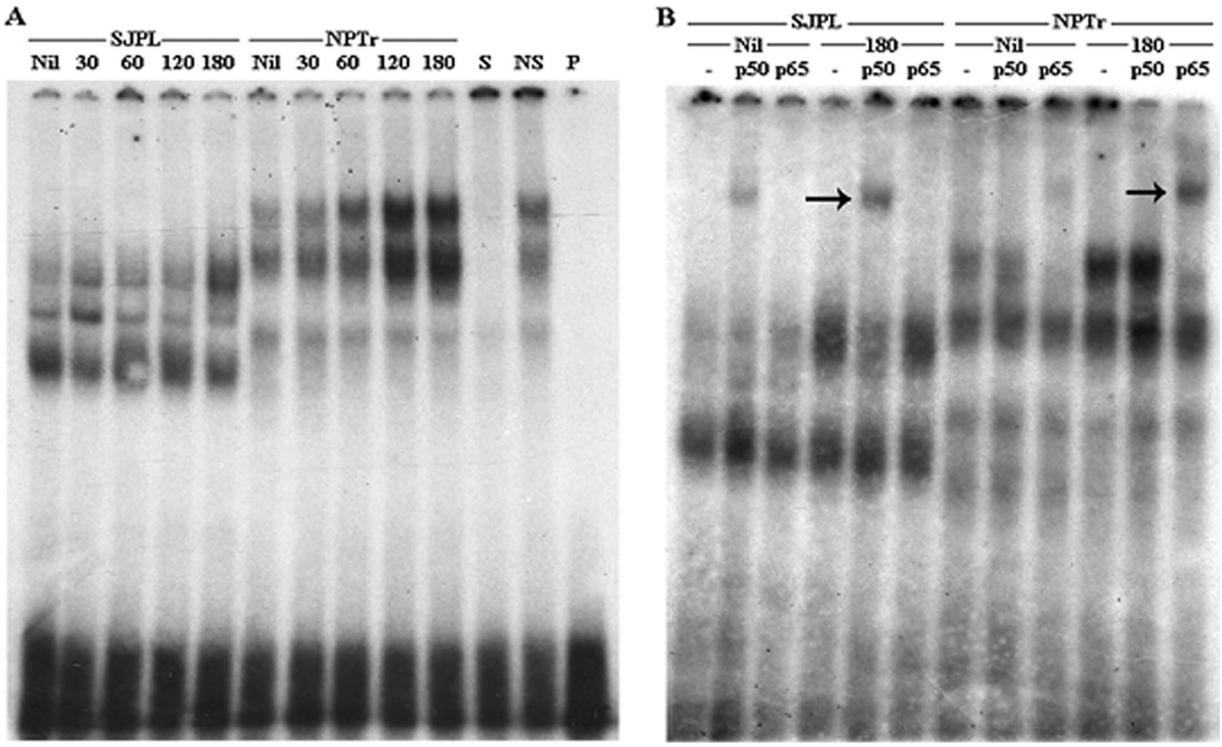

FIG. 4. EMSA (A) or supershift assay (B) performed on nuclear proteins of SJPL and NPTr cells following an incubation (30 to 180 min) with *A. pleuropneumoniae* S4074 or no treatment for the control (Nil). For controls, proteins were incubated with specific oligonucleotides (S) and nonspecific oligonucleotides (NS). The probe alone was also loaded on the gel (P). For the supershift assay (B), proteins were incubated with p50 antibodies (p50), p65 antibodies (p65), or no antibodies (-). Arrows demonstrate the subunit band shifts (B).

phenethyl ester in the NPTr cells, IL-8 concentrations decreased to basal levels (data not shown). This demonstrates that the production of IL-8 observed for the NPTr cells is indeed due to the induction of NF-κB.

To further investigate the mechanism of NF-κB induction in both cell lines, we performed an EMSA on cells pretreated with an IRAK1/4 inhibitor. IRAK1/4 is recruited by the MyD88 protein immediately after Toll receptor activation at the beginning of the NF-κB pathway (27). The level of NF-κB induction in comparison to that of noninhibited cells consequently demonstrated indirectly if the activation of Toll-like receptors by the bacterium is responsible for this induction. Our EMSA results indicate that for the SJPL cells, NF-κB induction occurs through the Toll receptor pathway (data not shown), but for the NPTr cells, NF-κB induction occurs through a different pathway.

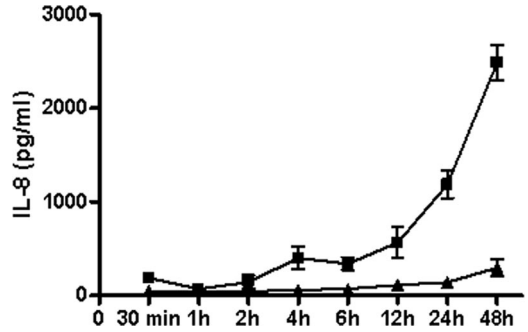

FIG. 5. Production of IL-8 by NPTr cells following an induction with heat-killed *A. pleuropneumoniae* S4074 (■) or when not stimulated (▲).

***A. pleuropneumoniae* transcriptomic profiling.** To assess the transcriptional response of *A. pleuropneumoniae* to both planktonic life over and adherence to SJPL cells, transcript profiling experiments using DNA microarrays were performed after an incubation time of 3 h. Overall, 170 genes were significantly differentially expressed during planktonic growth (Tables 2 and 3), with this number dropping to 131 during adhesion to SJPL cells (Tables 4 and 5). While some genes showed similar patterns of expression during the two conditions, 150 were differentially expressed(see Table S3 in the supplemental material).

The genes that showed the highest level of upregulation during planktonic growth belonged to the "Energy metabolism" functional class, and this class was also the most affected, with 24 out of the 82 upregulated genes. Surprisingly, most of these genes are involved in anaerobic respiration. Various enzymes involved in anaerobic respiration using alternative electron acceptors were upregulated: genes encoding subunits of the formate dehydrogenase (*fdxG*, and *fdnHI*) and nitrate reductase (*nrfABC*), which are essential for anaerobic respiration on nitrate (35, 62), and genes encoding subunits of the fumarate reductase (*frdACD*), which allows fumarate to serve as a terminal electron acceptor (10), were all upregulated. Furthermore, the genes *pgi*, *fbp*, and *pykA*, which encode three enzymes involved at various steps of glycolysis, glucose-6-phosphate isomerase, fructose-1,6-bisphosphatase, and pyruvate

TABLE 2. *A. pleuropneumoniae* genes which are upregulated during planktonic life over SJPL cells[a]

Locus tag	Gene	Description	Fold change
Hypothetical/unclassified/unknown			
APL_1839	*udp*	COG2820: uridine phosphorylase, probable outer membrane protein, possible efflux protein	3.937
APL_1833		COG2717: predicted membrane protein, conserved hypothetical protein	3.388
APL_1435		Unassigned protein	3.214
APL_1285		Hypothetical protein	2.894
APL_0145		COG1611: predicted Rossmann fold nucleotide-binding protein	2.726
APL_1976	*yedF*	COG0425: predicted redox protein, regulator of disulfide bond formation	2.669
APL_0116		Hypothetical protein	2.523
APL_0093		DUF1260 domain-containing protein	2.020
APL_1374		Unassigned protein	1.946
APL_0465		DUF74 domain-containing protein	1.943
APL_1919		Predicted enzyme related to aldose 1 epimerase	1.939
APL_1138		DUF526 domain-containing protein	1.933
APL_0443		COG5295: autotransporter adhesin	1.918
APL_1656		COG0561: predicted hydrolases of the HAD superfamily	1.842
APL_1203		DUF479 domain-containing protein, hypothetical protein	1.811
APL_1609		DUF533 domain-containing protein	1.724
APL_1881		Putative carbamoylphosphate synthase large subunit	1.703
APL_1244		Hypothetical protein	1.555
Biosynthesis of cofactors			
APL_1622	*cbiM*	Predicted ABC cobalt transport permease protein CbiM	2.419
APL_0931	*iscS*	Cysteine desulfurase, iron-sulfur cluster assembly	2.374
APL_0930	*nifU*	NifU-like protein, involved in Fe-S cluster formation	2.011
APL_1555	*hemL*	Glutamate-1-semialdehyde 2,1-aminomutase	1.619
Energy metabolism			
APL_1832		COG2041: sulfite oxidase and related enzymes	13.073
APL_0892	*fdxG*	Formate dehydrogenase, nitrate inducible, major subunit	12.558
APL_0895	*fdnI*	Formate dehydrogenase, cytochrome b_{556} subunit	10.946
APL_0894	*fdxH*	Formate dehydrogenase, iron-sulfur subunit	6.0988
APL_0687	*dld*	D-Lactate dehydrogenase	5.442
APL_0100	*nrfA*	Ammonia-forming cytochrome c_{552} nitrite reductase	5.039
APL_0106	*putA*	Bifunctional protein PutA	4.634
APL_0101	*nrfB*	Nitrate reductase, cytochrome-*c*-type protein	4.295
APL_1091	*aspA*	Aspartate ammonia lyase	4.254
APL_1528	*frdC*	Fumarate reductase subunit C	3.713
APL_1137	*pgi*	Glucose-6-phosphate isomerase	3.136
APL_1959	*adhI*	Alcohol dehydrogenases 1	2.992
APL_1414	*mqo*	Putative malate:quinone oxidoreductase	2.802
APL_1379	*ccp*	Cytochrome *c* peroxidase	2.796
APL_1450	*fbp*	Fructose-1,6-bisphosphatase	2.528
APL_1529	*frdA*	Fumarate reductase, flavoprotein subunit	2.420
APL_0187	*pykA*	Pyruvate kinase	2.322
APL_1197		3-Hydroxyacid dehydrogenase	2.270
APL_0102	*nrfC*	Nitrate reductase	2.250
APL_1526	*frdD*	Fumarate reductase subunit D	2.178
APL_0486	*maeA*	Malic enzyme (NADP dependent)	2.074
APL_1674	*dmsA*	Anaerobic dimethylsulfoxide reductase chain A precursor	1.934
APL_0483		Predicted nitroreductase	1.912
APL_0084	*trxB*	Thioredoxin reductase	1.486
Transport and binding proteins: cations and iron			
APL_1265	*copA*	Copper-transporting P-type ATPase	1.518
Transport and binding proteins: others			
APL_0107	*putP*	Na^+/proline symporter	6.218
APL_1173	*pnuC*	Nicotinamide mononucleotide transporter	2.448
APL_0377	*glpT*	Glycerol-3-phosphate transporter	2.331
APL_1254		COG0471: di- and tricarboxylate transporters	2.237
APL_1319	*ptsB*	PTS system sucrose-specific EIIBC component	2.206
APL_0447	*lctP*	L-Lactate permease	2.204
APL_0262	*modA*	Molybdate-binding periplasmic protein precursor	2.049
APL_1620	*cbiO*	Predicted ABC-type cobalt transport system, ATPase component	1.902

Continued on following page

TABLE 2—*Continued*

Locus tag	Gene	Description	Fold change
APL_1627		Putative di- and tricarboxylate transporters	1.876
APL_1624	*cbiK*	Putative periplasmic binding protein CbiK	1.823
APL_1902	*yrhG*	COG2116: formate/nitrite family of transporters	1.718
APL_1371	*ccmB*	Heme exporter protein B, cytochrome-*c*-type biogenesis protein	1.596
Regulatory functions			
APL_108	*iclR*	Putative HTH-type transcriptional regulator	2.832
APL_0395	*rseA*	Putative sigma E factor negative regulatory protein	2.260
APL_0823	*glpR*	Glycerol-3-phosphate regulon repressor	2.175
APL_0997	*lacZ*	Beta-galactosidase	1.654
Transcription			
APL_1475	*rpoD*	RNA polymerase sigma 70 factor	2.135
APL_0560	*rhlB*	ATP-dependent RNA helicase RhlB	1.911
Purines, pyrimidines, nucleosides, and nucleotides			
APL_0646	*cpdB*	2′,3′-cyclic-nucleotide 2′-phosphodiesterase precursor	2.087
Protein fate			
APL_0742	*degS*	Protease DegS precursor	1.768
APL_0871	*pepE*	Peptidase E	1.686
Protein synthesis			
APL_0484	*rimK*	Ribosomal protein S6 modification enzyme	3.093
APL_0146	*dusA*	tRNA-dihydrouridine synthase A	2.456
Cellular processes			
APL_0004	*sodC*	Cu/Zn superoxide dismutase precursor	3.003
APL_0251	*sodA*	Manganese superoxide dismutase	2.356
APL_1241		Probable carbon starvation protein A, predicted membrane protein	2.098
APL_1405	*oapA*	Cell envelope opacity-associated protein A	1.793
Cell envelope			
APL_1494	*ftpA*	DNA-binding ferritin-like protein (oxidative damage protectant), fine-tangled pilus major subunit (24-kDa surface protein)	6.378
Fatty acid and phospholipid metabolism			
APL_0397	*lcfA*	Acyl-CoA synthetases (AMP forming)/AMP-acid ligases II[b]	1.746
Mobile and extrachromosomal element functions			
APL_1501		Transposase	2.078
APL_0990		Transposase	1.814
APL_0985		Transposase	1.680
DNA metabolism			
APL_1143	*recA*	RecA recombinase	1.491
Central intermediary metabolism			
APL_0109		Possible 5-formyltetrahydrofolate cycloligase	2.607
APL_0375	*glpK*	Glycerol kinase	2.316

[a] Eighty-two genes.
[b] CoA, coenzyme A.

kinase, respectively, showed an increase in transcription. Two dehydrogenases, alcohol dehydrogenase I (encoded by *adhI*) and malate:quinone oxidoreductase (encoded by *mqo*), are also involved in anaerobic respiration, the latter being controlled by the ArcA-ArcB two-component system (59). The genes *aspA* and *dmsA* were also upregulated. The "Transport and binding proteins" class was the second most affected, with 12 upregulated genes. Genes involved in the transport of L-lactate (*lctP*), formate and nitrite (*yrhG*), sucrose (*ptsB*), and glycerol (*glpT*) were all induced, as was the gene *modA*, which encodes a periplasmic protein involved in the ABC transport of molybdate (25). The gene APL_0443, coding for a putative autotransporter adhesin, showed a 1.9-fold induction.

Genes downregulated during planktonic growth mostly belonged to the "Protein synthesis" and "Transport and binding proteins: cations and iron" functional classes. The *hgbA* hemoglobin receptor gene and its *hugZ* heme utilization protein cotranscript were downregulated, and other well-established

TABLE 3. *A. pleuropneumoniae* genes which are downregulated during planktonic life over SJPL cells[a]

Locus tag	Gene	Description	Fold change
Hypothetical/unclassified/unknown			
APL_1387		Predicted metal-binding, possibly nucleic acid-binding protein	−2.431
APL_0053	*typA*	Predicted membrane GTPase involved in stress response	−2.386
APL_0173		Hypothetical cytosine deaminase and related metal-dependent hydrolases	−2.056
APL_1863		Predicted glycosyltransferase	−2.027
APL_1956		Hypothetical protein	−2.000
APL_0936		Putative integral membrane protein	−1.829
Energy metabolism			
APL_1849	*lldD*	L-Lactate dehydrogenase (FMN dependent) and related alpha-hydroxy acid dehydrogenases	−3.284
APL_0592	*guaA*	GMP synthase	−2.629
APL_1219	*fldA*	Flavodoxin	−2.276
Transport and binding proteins: cations and iron			
APL_1047	*hgbA*	Hemoglobin-binding protein A precursor	−9.346
APL_1571	*tonB1*	Periplasmic energy transducing protein TonB1	−5.319
APL_1952		Outer membrane receptor protein, mostly Fe transport	−3.517
APL_0077	*exbD2*	Energy transducing protein ExbD2	−3.499
APL_1953		Outer membrane receptor protein, mostly Fe transport	−2.874
APL_0670		Putative Fe^{2+}/Pb^{2+} permease	−2.406
APL_1048	*hugZ*	Heme utilization protein	−2.387
APL_0272	*yfeA*	Iron (chelated) ABC transporter, periplasmic binding protein	−2.339
APL_0271	*yfeB*	putative chelated iron transport system ATP-binding protein	−2.251
APL_0714		Putative ABC-type enterochelin transport system, periplasmic component	−2.178
APL_1954		Outer membrane receptor proteins, mostly Fe transport	−2.163
APL_0715		COG4606: ABC-type enterochelin transport system, permease component	−1.993
APL_1955		Outer membrane receptor proteins, mostly Fe transport	−1.891
APL_0717		COG4604: ABC-type enterochelin transport system, ATPase component	−1.760
APL_0127	*yfeD*	Putative iron transport system membrane protein	−1.718
Transport and binding proteins: others			
APL_0300	*tolQ*	Colicin transport protein	−2.584
APL_1392	*ptnC*	Mannose permease component IIC	−2.135
APL_1393	*ptnD*	Mannose permease component IID	−2.043
APL_1584	*cpxB*	Capsule polysaccharide export inner membrane protein	−1.863
APL_1585	*cpxA*	Capsule polysaccharide export ATP-binding protein	−1.572
APL_1583	*cpxC*	Capsule polysaccharide export inner membrane protein	−1.549
Transcription			
APL_0638	*nusA*	Transcription elongation factor	−3.997
APL_0577	*pnp*	Polyribonucleotide nucleotidyltransferase	−2.375
APL_0757	*rnb*	Exoribonuclease II	−1.665
APL_0543	*rnc*	RNase III	−1.539
Purines, pyrimidines, nucleosides, and nucleotides			
APL_0148	*rnr1*	Ribonucleotide reductase, alpha subunit	−2.556
APL_0593	*guaB*	Inosine-5′-monophosphate dehydrogenase	−2.474
APL_0147		Ribonucleotide reductase, beta subunit	−2.438
APL_0255	*gpt*	Xanthine phosphoribosyltransferase	−2.316
APL_0661	*purK*	Phosphoribosylaminoimidazole carboxylase ATPase subunit	−2.091
APL_1172	*purD*	Phosphoribosylamine-glycine ligase	−1.883
APL_2018	*purC*	Phosphoribosylaminoimidazole-succinocarboxamide synthase	−1.717
APL_0834	*udk*	Uridine kinase	−1.396
Protein fate			
APL_1507	*tig*	FKBP-type peptidyl-prolyl *cis-trans* isomerase (trigger factor)	−3.849
APL_0364	*Ssa1*	Autotransporter serine protease	−2.279
Protein synthesis			
APL_1718	*rplK*	50S ribosomal protein L11	−5.061
APL_0639	*infB*	Translation initiation factor 2 (IF-2)	−4.243
APL_1774	*rplF*	Ribosomal protein L6	−3.954
APL_1720	*rplJ*	Ribosomal protein L10	−3.833

Continued on following page

TABLE 3—*Continued*

Locus tag	Gene	Description	Fold change
APL_1558	*rpsT*	30S ribosomal protein S20	−3.720
APL_1765	*rplV*	50S ribosomal protein L22	−3.039
APL_0566	*rpsB*	30S ribosomal protein S2	−2.842
APL_1400	*rpsG*	30S ribosomal protein S7	−2.714
APL_0487	*rplY*	50S ribosomal protein L25 (general stress protein Ctc)	−2.364
APL_1762	*rplW*	50S ribosomal protein L23	−2.330
APL_1763	*rplB*	50S ribosomal protein L2	−2.265
APL_1761	*rplD*	50S ribosomal protein L4	−2.254
APL_0223	*infC*	Translation initiation factor 3 (IF-3)	−2.192
APL_1773	*rpsH*	30S ribosomal protein S8	−2.100
APL_1775	*rplR*	50S ribosomal protein L18	−2.020
APL_0399	*ksgA*	Dimethyladenosine transferase (rRNA methylation)	−1.950
APL_1401	*rpsL*	30S ribosomal protein S12	−1.914
APL_1972	*rpmG*	50S ribosomal protein L33	−1.902
APL_0040	*yhbZ*	Hypothetical GTP-binding protein	−1.721
APL_1228	*infA*	Translation initiation factor 1	−1.716
APL_0678	*efp*	Translation elongation factor P	−1.708
APL_1781	*rpsM*	30S ribosomal protein S13	−1.705
APL_1383		tRNA (guanine-*N*(7)-)-methyltransferase	−1.688
APL_0641	*truB*	tRNA pseudouridine synthase B	−1.660
APL_1476	*tyrS*	Tyrosyl-tRNA synthetase	−1.646
APL_1789	*rplS*	50S ribosomal protein L19	−1.521
Cellular processes			
APL_0669		Predicted iron-dependent peroxidase	−2.630
APL_1443	*apxIB*	Toxin RTX-I translocation ATP-binding protein	−1.753
Cell envelope			
APL_0933	*ompP1*	Putative long-chain-fatty-acid transport protein precursor	−8.199
APL_0651	*galU*	UTP-glucose-1-phosphate uridylyltransferase	−2.114
APL_1989		Predicted membrane protein	−1.951
APL_1071		Putative xanthine/uracil permease	−1.817
Fatty acid and phospholipid metabolism			
APL_1864	*accB*	Biotin carboxyl carrier protein of acetyl-CoA carboxylase[b]	−2.570
APL_1865	*accC*	Biotin carboxylase	−2.444
APL_1889	*fabA*	3-Hydroxydecanoyl-(acyl carrier protein) dehydratase	−2.426
APL_1385	*plsX*	Fatty acid/phospholipid biosynthesis enzyme PlsX	−1.922
Amino acid biosynthesis			
APL_0194	*aroK*	Shikimate kinase	−2.401
APL_1499	*thrC*	Threonine synthase	−2.083
DNA metabolism			
APL_0190	*fis*	Factor for inversion stimulation (Fis), transcriptional activator	−2.209
APL_0074	*recR*	Recombinational DNA repair protein (RecF pathway)	−1.634
Central intermediary metabolism			
APL_1508		Putative rhodanese-related sulfurtransferase	−2.860
APL_0175	*dksA*	DnaK suppressor protein	−1.845
APL_0349	*glgA*	Glycogen synthase	−1.505

[a] Eighty-eight genes.
[b] CoA, coenzyme A.

iron acquisition-related genes included *tonB1* and *exbD2*. These genes are cotranscribed with other members of the TonB1 (*exbB1*, *exbD1*, *tbpA*, and *tbpB*) and TonB2 (*exbB2* and *exbD2*) energy transduction system (7), but these were not identified in our study. At this time, the genes *exbB1*, *exbD1*, and *tbpB* are not present on AppChip1, and the gene *tbpA* was not downregulated. The genes *exbB2* and *tonB2*, however, exhibit a twofold average downregulation, but variations between chips might have caused these to be ignored by our very stringent analysis parameter (false discovery rate = 0%). A high number of genes that were identified for the first time in *A. pleuropneumoniae* in our previous transcript profiling experiment under iron restriction (13) were also downregulated. The open reading frames APL_1952 to APL_1955, which code for a putative second hemoglobin receptor system and are likely transcriptionally linked, were repressed, as were the genes APL_0714-APL_0715-APL_0717, encoding a putative ABC-type siderophore transport system, and the genes *yfeABD*,

TABLE 4. *A. pleuropneumoniae* genes which are upregulated during adherence to SJPL cells[a]

Locus tag	Gene	Description	Fold change
Hypothetical/unclassified/unknown			
APL_0568		Hypothetical membrane protein	3.083
APL_1459		Hypothetical protein	2.882
APL_1690		Predicted periplasmic/secreted protein	2.609
APL_1471		Putative sugar transferase	2.450
APL_1380		Uncharacterized conserved protein	2.310
APL_2002		Hypothetical protein	2.301
APL_0750		MscS family protein	2.181
APL_1575		Hypothetical protein	1.940
APL_1103		Predicted inner membrane protein	1.844
APL_1854	*pqiA*	Uncharacterized paraquat-inducible protein A	1.746
APL_0217		Hypothetical protein	1.640
Biosynthesis of cofactors			
APL_0776	*ispE*	4-Diphosphocytidyl-2*C*-methyl-D-erythritol 2-phosphate synthase	2.913
Energy metabolism			
APL_1849	*lldD*	L-Lactate dehydrogenase	6.756
APL_1820	*rpe*	D-Ribulose-phosphate-3 epimerase	6.687
APL_1191	*namA*	NADPH dehydrogenase	4.524
APL_1331	*hyaA*	Hydrogenase 2 small chain precursor	3.366
APL_1685	*fucK*	L-Fuculokinase	3.195
APL_1689	*fucO*	Probable alcohol dehydrogenase, class IV	2.887
APL_1684	*fucI*	L-Fucose isomerase	2.812
APL_1333	*hybB*	Putative Ni/Fe hydrogenase 2 *b*-type cytochrome component	2.796
APL_1019	*kdgK*	2-Dehydro-3-deoxygluconokinase	2.334
APL_0896	*fdhE*	Formate dehydrogenase accessory protein FdhE	2.007
Transport and binding proteins: cations and iron			
APL_1793	*fecE*	Fe(III) dicitrate ABC transporter, ATP-binding protein	6.113
APL_1955		Outer membrane receptor proteins, mostly Fe transport	3.271
APL_1981	*corA*	Magnesium transport protein CorA	3.001
APL_0077	*exbD2*	Energy transducing protein ExbD2	2.346
Transport and binding proteins: others			
APL_0066	*dppC*	Dipeptide transport system, permease components	12.073
APL_0870		Putative C_4-dicarboxylate transporter	6.308
APL_1713		Putative oligopeptide transporter	4.639
APL_0191		Predicted Na^+-dependent transporters of the SNF family	4.638
APL_0309	*yheS*	Putative ABC transporter ATP-binding protein YheS	2.331
APL_1848	*cysA*	Sulfate/thiosulfate import ATP-binding protein CysA	1.938
APL_1249	*sapF*	Peptide transport system ATP-binding protein SapF	1.858
APL_0260	*modC*	Molybdenum import ATP-binding protein ModC	1.799
APL_0582	*sotB*	Putative efflux transporter	1.773
Regulatory functions			
APL_1099		Organic radical activating enzymes	7.175
APL_1962	*hflX*	GTP-binding protein HflX	2.005
Transcription			
APL_0176	*pcnB*	Putative poly(A) polymerase	2.566
Purines, pyrimidines, nucleosides, and nucleotides			
APL_0775	*prsA*	Ribose-phosphate pyrophosphokinase	8.463
APL_0425	*purF*	Amidophosphoribosyltransferase	1.812
Protein fate			
APL_1742	*srp54*	Signal recognition particle protein (sigma 54 like)	6.861
APL_1905	*dnaJ*	Chaperone protein DnaJ	3.383
APL_1330	*hypF*	Carbamoyltransferase HypF	2.080
Protein synthesis			
APL_0034	*engD*	GTP-dependent nucleic acid-binding protein EngD	17.924
APL_0575	*deaD*	Superfamily II DNA and RNA helicases	6.254

Continued on following page

TABLE 4—*Continued*

Locus tag	Gene	Description	Fold change
APL_0487	*rplY*	50S ribosomal protein L25 (general stress protein Ctc)	3.429
APL_1325		Putative 2-methylthioadenine synthetase	2.357
APL_1112	*rumA*	23S rRNA (uracil-5-)-methyltransferase RumB	2.145
APL_0853		Methionine synthase II (cobalamin independent)	2.078
Cellular processes			
APL_1922	*pgaB*	Biofilm PGA synthesis lipoprotein PgaB precursor	7.257
APL_0011	*ftsL*	Cell division protein FtsL	3.349
APL_1923	*pgaC*	Biofilm PGA synthesis *N*-glycosyltransferase PgaC	2.454
Cell envelope			
APL_0551	*tadB*	Tight adherence protein B	2.453
APL_1841	*murI*	Glutamate racemase	2.340
APL_0016	*murD*	UDP-*N*-acetylmuramoy-L-alanine-D-glutamate synthetase	2.113
APL_1598	*mrdB*	Rod-shape determining protein	2.096
APL_0419	*lgtF*	UDP-glucose-lipooligosaccharide glucosyltransferase	1.929
APL_1554	*wecA*	Putative undecaprenyl-phosphate α-*N*-acetylglucosaminyl 1-phosphate transferase	1.577
APL_0555	*rcpA*	Rough colony protein A	1.559
Fatty acids and phospholipids metabolism			
APL_1864	*accB*	Biotin carboxyl carrier protein of acetyl-CoA carboxylase[b]	8.665
APL_1865	*accC*	Biotin carboxylase	4.016
APL_0887	*fadI*	3-ketoacyl-CoA thiolase	3.675
Amino acids biosynthesis			
APL_0320	*metC*	Cystathionine beta-lyase	9.278
APL_0099	*ilvG*	Acetolactate synthase isozyme II large subunit	6.897
APL_1452	*serA*	D-3-Phosphoglycerate dehydrogenase	3.896
APL_0469	*trpB*	Tryptophan synthase beta chain	3.274
APL_0139	*leuC*	3-Isopropylmalate dehydratase large subunit 2	3.253
APL_1951	*proA*	Gamma-glutamyl phosphate reductase	2.846
APL_1147	*trpG*	Putative anthranilate synthase component II	2.723
APL_0249	*thrB*	Homoserine kinase	2.459
APL_1125		Putative cysteine desulfurase	2.068
DNA metabolism			
APL_1196		Type I site-specific restriction-modification system, R subunit	3.251
APL_1194		Type I restriction-modification system, methyltransferase subunit	2.816
APL_1146	*rmuC*	DNA recombination protein RmuC homolog	2.462
APL_0874	*holA*	DNA polymerase III, delta subunit	2.022
APL_0287	*hsdM*	Putative type I restriction-modification system, methyltransferase subunit	2.005
Central intermediary metabolism			
APL_2045	*sseA*	Probable thiosulfate sulfurtransferase	1.942
APL_1843	*cysJ*	Sulfite reductase [NADPH] flavoprotein alpha component	1.780

[a] Seventy-nine genes.
[b] CoA, coenzyme A.

likely responsible for the ABC-like periplasmic binding protein-dependent transport of chelated iron and possibly manganese. The genes *cpxABC*, coding for the capsule polysaccharide ABC-type export system, were also all downregulated, along with the gene *ssa1*, encoding a putative autotransporter serine protease.

Interestingly, some genes potentially involved in adhesion and biofilm biosynthesis were upregulated during adherence to SJPL cells. The genes *rcpA* and *tadB*, which belong to a large operon of 14 genes, were upregulated, as were the genes *pgaBC*, involved in poly-β-1,6-*N*-acetyl-D-glucosamine biofilm biosynthesis. A small number of genes involved in iron acquisition were also upregulated, the most notable being *fecE* and APL_1955. Once again, genes involved in anaerobic respiration were shown to be upregulated. Other enzyme genes coding for hydrogenases (*hyaA* and *hybB*) or dehydrogenases (*lldD* and *fdhE*) involved in energy metabolisms also showed upregulation. The gene *fucO*, essential for the anaerobic degradation of fucose, and the genes *fucI* and *fucK*, (11), involved in the general fucose degradation pathway, were also upregulated.

Only 52 genes were identified as downregulated, and most of them belong to the "Energy metabolism" functional class. The six enzymes which catalyze the first six steps of glycolysis (encoded by *gapA*, *pgk*, *fbp*, *tpiA*, *pgi*, and *fba*) were downregulated, as was the gene *maeA*, responsible for the first step of gluconeogenesis, and the gene *tktA*, which links glycolysis to

TABLE 5. *A. pleuropneumoniae* genes which are downregulated during adherence to SJPL cells[a]

Locus tag	Gene	Description	Fold change
Hypothetical/unclassified/unknown			
APL_1887		Esterase domain-containing protein	−6.273
APL_1284		Putative DNA-binding protein	−3.076
APL_0049		Hypothetical protein	−2.982
APL_0970		Hypothetical protein	−2.980
APL_1100		Hypothetical protein	−2.928
APL_1437		Hypothetical protein	−2.751
APL_0116		Hypothetical protein	−2.566
APL_0389	*ompP4*	Lipoprotein E precursor, predicted secreted acid phosphatase	−2.509
APL_0704		Potential type III restriction enzyme	−2.293
APL_1365	*Hly*	Hypothetical protein	−2.174
APL_0110		Hypothetical protein	−2.144
APL_1396		Hypothetical protein	−2.125
APL_0756		Hypothetical protein	−2.098
APL_0889		Hypothetical protein	−1.757
Energy metabolism			
APL_0434	*gapA*	Glyceraldehyde-3-phosphate dehydrogenase	−4.981
APL_0892	*fdxG*	Formate dehydrogenase, nitrate-inducible, major subunit	−4.853
APL_0771	*lpdA*	Dihydrolipoyl dehydrogenase	−4.765
APL_1379	*ccp*	Cytochrome c peroxidase	−4.447
APL_0983	*tktA*	Transketolase 2	−3.790
APL_0894	*fdxH*	Formate dehydrogenase, iron-sulfur subunit	−3.627
APL_1251	*pgk*	3-Phosphoglycerate kinase	−3.625
APL_1450	*fbp*	Fructose-1,6-bisphosphatase	−3.315
APL_0181	*gloA*	Lactoylglutathione lyase	−3.046
APL_1925	*tpiA*	Triosephosphate isomerase	−3.023
APL_1091	*aspA*	Aspartate ammonia-lyase	−2.722
APL_0688	*torZ*	Trimethylamine-*N*-oxide reductase precursor	−2.687
APL_1011	*adh2*	Aldehyde-alcohol dehydrogenase 2	−2.642
APL_0772	*aceF*	Dihydrolipoyllysine-residue acetyltransferase component of pyruvate dehydrogenase complex (E2)	−2.620
APL_1137	*pgi*	Glucose-6-phosphate isomerase	−2.595
APL_0486	*maeA*	NADP-dependent malic enzyme	−2.416
APL_1526	*frdD*	Fumarate reductase subunit D	−2.267
APL_0101	*nrfB*	Nitrate reductase, cytochrome-*c*-type protein	−2.231
APL_1250	*fba*	Fructose bisphosphate aldolase	−2.124
Transport and binding proteins: others			
APL_1620	*cbiO*	Predicted ABC-type cobalt transport, ATPase component	−2.108
APL_0447	*lctP*	Putative L-lactate permease	−2.068
APL_0719		Putative phosphate permeases	−1.816
APL_0791		Transmembrane transport protein-permease	−1.702
Regulatory functions			
APL_0656	*hlyX*	Regulatory protein HlyX	−2.727
APL_0629	*cpxR*	Transcriptional regulatory protein CpxR	−2.367
Purines, pyrimidines, nucleosides, and nucleotides			
APL_0769	*ushA*	UshA precursor	−3.470
APL_0646	*cpdB*	2′,3′-Cyclic-nucleotide 2′-phosphodiesterase precursor	−2.778
APL_1014	*deoD*	Purine-nucleoside phosphorylase	−2.247
Protein fate			
APL_1154		Putative zinc protease	−2.401
APL_1456	*slyD*	FkbP-type peptidyl-prolyl *cis-trans* isomerase	−2.313
Protein synthesis			
APL_0740	*rpsA*	30s ribosomal protein S1	−1.608
Cellular processes			
APL_1445	*apxIC*	RTX-I toxin-activating lysine-acyltransferase ApxIC	−4.117
APL_0956	*apxIIA*	RTX-II toxin determinant A	−4.052
APL_0004	*sodC*	Superoxide dismutase (Cu/Zn) precursor	−3.193
Cell envelope			
APL_1494	*ftpA*	COG0783: DNA-binding ferritin-like protein (oxidative damage protectant)	−4.223
APL_0652	*manB*	Phosphomannomutase	−3.375
Central intermediary metabolism			
APL_0645	*ackA*	Acetate kinase	−3.190
APL_1899	*ppa*	Inorganic pyrophosphatase	−2.207

[a] Fifty-two genes.

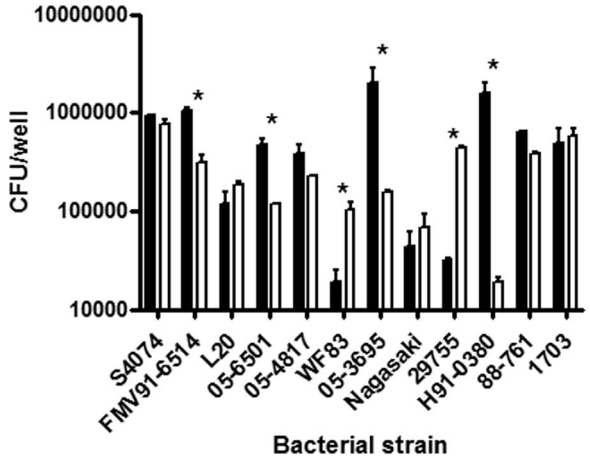

FIG. 6. Adherence of 12 members of the *Pasteurellaceae* to the SJPL (filled bars) or NPTr (empty bars) cell line after 3 h of incubation. The strains include *A. pleuropneumoniae* serotype 1 S4074 and FMV91-6514, *A. pleuropneumoniae* serotype 5b L20 and 05-6501, *A. pleuropneumoniae serotype* 5a 05-4817, *A. pleuropneumoniae* serotype 7 WF83 and 05-3695, *H. parasuis* serotype 5 Nagasaki and 29755, *A. suis* serotype O2/K2 H91-0380, and *P. multocida* capsular type A 88-761 and capsular type D 1703. Asterisks represent statistical differences ($P < 0.05$) in adherence of the given strain between the two cell lines.

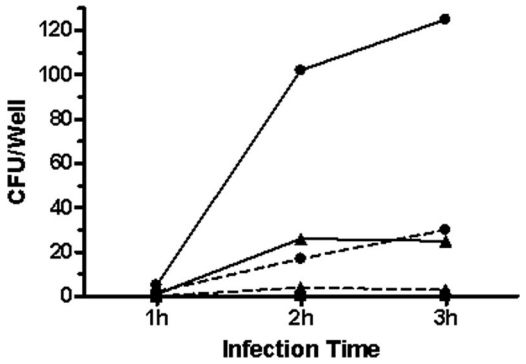

FIG. 7. Invasion by *A. pleuropneumoniae* S4074 (■), *H. parasuis* Nagasaki (▲), and *H. parasuis* 29755 (●) of SJPL (full line) or NPTr (dashed line) cells from 1 h to 3 h.

the pentose-phosphate pathway. *hlyX*, coding for the *A. pleuropneumoniae* FNR anaerobic global regulator homolog, was repressed 2.72-fold. The toxin genes *apxIC* and *apxIIA* also showed downregulation during adhesion to SJPL cells.

Adherence and invasion of *A. pleuropneumoniae* and other members of the *Pasteurellaceae*. Other serotypes of *A. pleuropneumoniae* and different swine-colonizing members of the *Pasteurellaceae* were tested using the adherence models. Differences in adherence were observed between strains for a given cell line and between the cell lines for a given strain (Fig. 6). We noticed that the field strains of *A. pleuropneumoniae* adhered significantly more to the cell lines than the reference strain of the same serotype. We also noticed that the level of adherence to a given cell line was strain dependent. Following the observation that all members of the *Pasteurellaceae* tested adhered to the cell lines, invasion tests were performed. *A. pleuropneumoniae* S4074 did not invade either cell line in our infection model, while the other members of the *Pasteurellaceae* tested showed invasion. *H. parasuis* showed the highest level of invasion, although at a reduced level compared to invasion seen with endothelial cells (Fig. 7) (60).

DISCUSSION

Using immortalized porcine lung and tracheal epithelial cells, we were able to study the host-pathogen interactions of *A. pleuropneumoniae.* In our models, *A. pleuropneumoniae* provoked cell death very rapidly through necrosis and not apoptosis. The presence of this bacterium causes many changes in the protein profiles of both epithelial cell lines. Indeed, using an antibody microarray as a rapid screening for differential protein expression, we were able to direct our efforts toward the NF-κB pathway, since numerous differentially expressed proteins were implicated in the NF-κB pathway, including IKKα and IKKβ. NF-κB consists of a homo- or heterodimer composed of the five mammalian Rel proteins, p65, c-Rel, p50, p52, and RelB (24), with the p50/p65 heterodimer being the most abundant and active of the NF-κB complexes (2). Out of the five subunits, only p65 (RelA), RelB, and c-Rel were found to contain the C-terminal transactivation domains essential for gene activation. In contrast, p50 and p52 do not possess the transactivation domains and therefore cannot act as transcriptional activators by themselves (39). Additionally, p50 and p52 are synthesized as precursor proteins that belong to the IκB family known as inhibitors of NF-κB, and homo- or heterodimers of p50 and p52 were also reported to repress κB site-dependent transcription in vivo (39). Interestingly, the p50 subunit was found to be induced in the SJPL cells but not in the NPTr cells after 3 h of incubation with *A. pleuropneumoniae* S4074, and inversely, the p65 subunit was induced in the NPTr cells only. It should be noted that the absence of detection of either p50 in the NPTr cells or p65 in the SJPL cells is not due to a weak bacterium-induced expression but is most probably due to the incapacity of the cell line to express the protein, since no basal level of expression was observed under unstimulated conditions for the subunits p50 in the NPTr cells and p65 in the SJPL cells. Those results suggest that in the absence of p65, inactive p50/p50 homodimers are more likely to form in the SJPL cells. The absence of IL-8 production by the SJPL cells might be explained by the weak NF-κB induction observed in the EMSAs but certainly correlates with the absence of the p65 subunit, necessary for binding to the IL-8 promoter. Previous studies have also shown that the binding affinity of p50 for the human IL-8 promoter is weak compared to the binding of the p65 subunit (38). Different pathways can activate NF-κB, the most frequent in gram-negative bacterial infection being the classical pathway through Toll-like receptor activation by LPS (44). We demonstrated that this is the case for the SJPL cells but not for the NPTr cells. A possibility is that an alternative pathway for NF-κB activation was used in the NPTr cells where IKKα homodimers are activated instead of the IKKβ in the classical pathway, leading to NF-κB2/p100 phosphorylation. This is a possibility, since this modification creates the production of p52 (44), a subunit which seems to be present in the stimulated NPTr cells, as seen in the EMSA, where a band slightly higher than p50 was detected, and since IKKα was upregulated in the NPTr antibody microarray. This pathway is generally triggered by TNF receptor family mem-

bers, such as LTβR, BAFF-R, CD40, and CD30 (44). Additional experiments are necessary, however, to confirm this theory.

The presence of the epithelial cells stimulated differential expression of many *A. pleuropneumoniae* genes. Although it was shown previously, with the evidence of a putative involvement in virulence of genes *dmsA* and *aspA*, that genes involved in anaerobic respiration might in fact be essential for full virulence of *A. pleuropneumoniae* in the host (3, 5, 30), it is still unclear why genes involved in anaerobic respiration are upregulated under our experimental conditions. While such a metabolic switch might be important in vivo to adapt to the lack of oxygen in the deep lung tissues, it should not be necessary in our experimental setup unless this apparent aerobic/anaerobic shift is controled by a host cell-associated factor rather than by oxygen sensors. In fact, it is worth noting that this metabolic shift does not seem to be complete, since genes involved in aerobic respiration are not downregulated. The upregulation of the gene *sodA*, coding for a cytoplasmic Mn superoxide dismutase (21), also seems to indicate that aerobic respiration is not stopped, since these cytoplasmic superoxide dismutases are specifically useful in removing superoxide anions generated during the course of aerobic respiration (54).

A gene with possible involvement in virulence was also identified. Locus tag APL_0443 is described as an autotransporter adhesin. This protein shows a region of high homology with the *A. actinomycetemcomitans* extracellular matrix protein adhesin A (EmaA), an oligomeric autotransporter with a YadA domain (57), and the putative *Mannheimia haemolytica* Hsf protein (40). In *Haemophilus influenzae* serotype b, Hsf (*Haemophilus* surface fibrils) is considered the major nonpilus adhesin (55) and was found to be associated with adherence to human epithelial cells (6, 26). Whether this putative *A. pleuropneumoniae* Hsf protein has these properties remains to be seen, but the upregulation of this gene during planktonic life over SJPL cells might hint to a possible role in the initial steps of *A. pleuropneumoniae* adhesion during infection.

The fact that iron, in DMEM, is available only in the form of ferric nitrate (12) might explain why iron acquisition systems are more expressed in cell-free DMEM than during planktonic growth. Experiments conducted in our laboratory have shown that ferric nitrate cannot support growth of *A. pleuropneumoniae* in an ethylenediamine dihydroxyphenyl acetic acid iron-restricted medium (13). Lysis of SJPL cells, leading to the release of the intracellular content of those cells in the medium, supplies the planktonic bacteria with more readily available sources of iron, for example, iron-sulfur clusters in the catalytic core of enzymes and ferritin-bound ferric iron.

Some genes with possible involvement in virulence also came up as downregulated during planktonic growth. Downregulation of the *cpxABC* operon during planktonic growth over SJPL cells might indicate that when in contact with host cells, *A. pleuropneumoniae* might wear a thinner polysaccharide layer in order to unmask some adhesins. Surprisingly, this downregulation of the *cpx* operon was not seen during adhesion to SJPL cells. Upon verification of changes during adhesion, only *cpxC* showed a low level of downregulation (−1.24), although this was not statistically significant. Repression of the gene *ssa1* was surprising, since this gene, also termed *aasP*, was shown to be expressed in vivo during the chronic stage of the disease (3). However, this gene was also shown to be iron responsive, as indicated by its upregulation during iron restriction (13). It might therefore simply follow the same trend as other iron-responsive genes which were downregulated during planktonic growth.

Our main focus, when looking at overexpressed genes during adherence to porcine lung epithelial cells, was to search for new potential adhesins. The genes *tadB* and *rcpA* are part of a large operon which, in *A. actinomycetemcomitans*, is composed of 14 genes (36) and mediates nonspecific adhesion to solid surfaces, whether they are biological surfaces or not (16). The genetic organization of the *A. pleuropneumoniae tad* locus is identical to that for *A. actinomycetemcomitans* (58). Although it is suspected that the *tad* genes might be transcribed as an operon, only two genes were identified as upregulated in our study. The 12 other genes are present on the microarray but are not significantly induced. Expression of the *tad* genes is responsible for the rough colony phenotype of *A. actinomycetemcomitans*, but smooth variants often arise after continued passage on rich medium (49) since mutations often appear in the promoter region of the gene *flp-1* (58). We suspect that this might also be the case for *A. pleuropneumoniae*, since most field isolates exhibit this rough colony phenotype while the reference strains are often smooth colony variants. As is the case for *A. actinomycetemcomitans*, the Tad proteins might play an important role for the colonization of the respiratory tract by *A. pleuropneumoniae*, but this will have to be further investigated. Other genes possibly involved in adhesion were also upregulated during adhesion to SJPL cells. The genes *pgaB* and *pgaC* are both involved in poly-β-1,6-*N*-acetyl-D-glucosamine (PGA) biofilm formation. A *pgaABCD* cluster is present in the App5b L20 genome, and the gene *pgaC* has been shown to be present in 15 reference strains (29). These results are interesting since the only components that have been clearly shown to be involved in *A. pleuropneumoniae* adhesion to lung surfaces to date are LPS (1, 8, 34, 45, 46).

The gene *hlyX* was downregulated during adhesion to SJPL cells. This gene, which encodes the *A. pleuropneumoniae* FNR anaerobic global regulator homolog, was shown to be important for the colonization and persistence of *A. pleuropneumoniae* in the respiratory tracts of swine (5). The repression of *hlyX* probably explains the repression of *aspA*, which is presumably regulated by HlyX, as well as the downregulation of a few other genes linked with anaerobic respiration (*fdxG*, *torZ*, *nrfB*, and *frdD*). Genes putatively regulated by HlyX have been shown to be induced by bronchoalveolar lavage fluid from infected pigs (30), and it is possible that *hlyX* expression follows the same pattern. Also, putative HlyX-regulated genes were upregulated during planktonic growth over SJPL cells.

ApxI and ApxII have been shown to be major virulence factors in *A. pleuropneumoniae*. Not much is known about transcriptional regulation of those toxins in *A. pleuropneumoniae.* Studies have shown that levels of oxygen do not influence the levels of ApxI and ApxII (33) and that the iron response regulator Fur seems to have variable effects depending on the calcium concentration in the culture medium (28). Under high calcium concentrations, Fur seemed to act as an activator of the *apxI* operon, while it seemed to act as a repressor under low calcium concentrations. A previous microarray study conducted under iron restriction showed that Fur does have an

effect on ApxI transcription (13). One would normally expect these toxins to be induced under conditions mimicking the in vivo environment, mostly after contact with epithelial cells. Downregulation of the genes *apxIC* and *apxIIA* was therefore intriguing. Perhaps smaller concentrations of RTX toxins are required when the bacteria are in close proximity to host cells, leading to the downregulation of the toxins following adherence.

Adherence is seen in both models for all *A. pleuropneumoniae* strains and serotypes tested. It is interesting to note that field strains adhere more to the cell lines than the reference strain of the same serotype. No invasion is noticed for *A. pleuropneumoniae*, even though close relatives, such as *A. actinomycetemcomitans* and *H. parasuis*, are known to be invasive (17, 42, 60).

Overall these results showed the efficacy of the models and allowed us to gain a great amount of knowledge of *A. pleuropneumoniae* host-pathogen interactions. Indeed, interaction of *A. pleuropneumoniae* with host epithelial cells seems to involve complex cross talk which results in the regulation of various bacterial genes. Many virulence genes were upregulated, including genes coding for the putative adhesins Hsf and poly-β-1,6-*N*-acetyl-D-glucosamine, while capsular polysaccharide-associated genes were downregulated, possibly exposing adhesins usually hidden by a thick capsule. Incubation with *A. pleuropneumoniae* then led, for both cell lines, to the induction of NF-κB. This is done through the activation of a Toll receptor for the SJPL cells but through an alternative pathway for the NPTr cells. The NPTr cells then secrete IL-8, which is known to attract neutrophils to the infection site, while the SJPL cells do not due to the absence of the p65 subunit of NF-κB. These models are a biologically relevant tool for studying porcine respiratory tract pathogens which could be further used, in the future, to evaluate the effect of a preinfection with agents such as mycoplasmas and viruses, often present with bacterial pathogens under field conditions.

ACKNOWLEDGMENTS

This work was supported by a discovery grant from the Natural Sciences and Engineering Research Council of Canada (DGPIN0003428) to M. Jacques and by a team grant from the FQRNT (2006-PR-106088) to M. Jacques and M. Gottschalk.

We thank M. Ferrari for the NPTr cell line and R. Webster for the SJPL cell line. We also acknowledge the contribution of Isabelle Gaucher and Geneviève Pelletier-Jacques.

REFERENCES

1. **Abul-Milh, M., S. E. Paradis, J. D. Dubreuil, and M. Jacques.** 1999. Binding of *Actinobacillus pleuropneumoniae* lipopolysaccharides to glycosphingolipids evaluated by thin-layer chromatography. Infect. Immun. **67:**4983–4987.
2. **Baeuerle, P. A., and T. Henkel.** 1994. Function and activation of NF-κB in the immune system. Annu. Rev. Immunol. **12:**141–179.
3. **Baltes, N., F. F. Buettner, and G. F. Gerlach.** 2007. Selective capture of transcribed sequences (SCOTS) of *Actinobacillus pleuropneumoniae* in the chronic stage of disease reveals an HlyX-regulated autotransporter protein. Vet. Microbiol. **123:**110–121.
4. **Baltes, N., and G. F. Gerlach.** 2004. Identification of genes transcribed by *Actinobacillus pleuropneumoniae* in necrotic porcine lung tissue by using selective capture of transcribed sequences. Infect. Immun. **72:**6711–6716.
5. **Baltes, N., M. N′Diaye, I. D. Jacobsen, A. Maas, F. F. Buettner, and G. F. Gerlach.** 2005. Deletion of the anaerobic regulator HlyX causes reduced colonization and persistence of *Actinobacillus pleuropneumoniae* in the porcine respiratory tract. Infect. Immun. **73:**4614–4619.
6. **Barenkamp, S. J., and J. W. St Geme III.** 1996. Identification of a second family of high-molecular-weight adhesion proteins expressed by non-typable *Haemophilus influenzae*. Mol. Microbiol. **19:**1215–1223.
7. **Beddek, A. J., B. J. Sheehan, J. T. Bosse, A. N. Rycroft, J. S. Kroll, and P. R. Langford.** 2004. Two TonB systems in *Actinobacillus pleuropneumoniae*: their roles in iron acquisition and virulence. Infect. Immun. **72:**701–708.
8. **Belanger, M., D. Dubreuil, J. Harel, C. Girard, and M. Jacques.** 1990. Role of lipopolysaccharides in adherence of *Actinobacillus pleuropneumoniae* to porcine tracheal rings. Infect. Immun. **58:**3523–3530.
9. **Blanchette, J., P. Pouliot, and M. Olivier.** 2007. Role of protein tyrosine phosphatases in the regulation of interferon-γ-induced macrophage nitric oxide generation: implication of ERK pathway and AP-1 activation. J. Leukoc. Biol. **81:**835–844.
10. **Cecchini, G., I. Schroder, R. P. Gunsalus, and E. Maklashina.** 2002. Succinate dehydrogenase and fumarate reductase from *Escherichia coli*. Biochim. Biophys. Acta **1553:**140–157.
11. **Chen, Y. M., Y. Zhu, and E. C. Lin.** 1987. The organization of the fuc regulon specifying L-fucose dissimilation in *Escherichia coli* K12 as determined by gene cloning. Mol. Gen. Genet. **210:**331–337.
12. **Conrad, D. R.** 2007. Ferric and ferrous iron in cell culture. Sigma-Aldrich Co., St. Louis, MO. http://www.sigmaaldrich.com/life-science/cell-culture/learning-center/media-expert/iron.html.
13. **Deslandes, V., J. H. Nash, J. Harel, J. W. Coulton, and M. Jacques.** 2007. Transcriptional profiling of *Actinobacillus pleuropneumoniae* under iron-restricted conditions. BMC Genomics **8:**72.
14. **Enriquez-Verdugo, I., A. L. Guerrero, J. J. Serrano, D. Godinez, J. L. Rosales, V. Tenorio, and M. de la Garza.** 2004. Adherence of *Actinobacillus pleuropneumoniae* to swine-lung collagen. Microbiology **150:**2391–2400.
15. **Ferrari, M., A. Scalvini, M. N. Losio, A. Corradi, M. Soncini, E. Bignotti, E. Milanesi, P. Ajmone-Marsan, S. Barlati, D. Bellotti, and M. Tonelli.** 2003. Establishment and characterization of two new pig cell lines for use in virological diagnostic laboratories. J. Virol. Methods **107:**205–212.
16. **Fine, D. H., D. Furgang, J. Kaplan, J. Charlesworth, and D. H. Figurski.** 1999. Tenacious adhesion of *Actinobacillus actinomycetemcomitans* strain CU1000 to salivary-coated hydroxyapatite. Arch. Oral Biol. **44:**1063–1076.
17. **Fives-Taylor, P., D. Meyer, and K. Mintz.** 1995. Characteristics of *Actinobacillus actinomycetemcomitans* invasion of and adhesion to cultured epithelial cells. Adv. Dent. Res. **9:**55–62.
18. **Foote, S. J., J. T. Bosse, A. B. Bouevitch, P. R. Langford, N. M. Young, and J. H. Nash.** 2008. The complete genome sequence of *Actinobacillus pleuropneumoniae* L20 (serotype 5b). J. Bacteriol. **190:**1495–1496.
19. **Frey, J.** 1995. Virulence in *Actinobacillus pleuropneumoniae* and RTX toxins. Trends Microbiol. **3:**257–261.
20. **Frey, J., R. Kuhn, and J. Nicolet.** 1994. Association of the CAMP phenomenon in *Actinobacillus pleuropneumoniae* with the RTX toxins ApxI, ApxII and ApxIII. FEMS Microbiol. Lett. **124:**245–251.
21. **Fridovich, I.** 1995. Superoxide radical and superoxide dismutases. Annu. Rev. Biochem. **64:**97–112.
22. **Fuller, T. E., R. J. Shea, B. J. Thacker, and M. H. Mulks.** 1999. Identification of in vivo induced genes in *Actinobacillus pleuropneumoniae*. Microb. Pathog. **27:**311–327.
23. **Gelfanova, V., E. J. Hansen, and S. M. Spinola.** 1999. Cytolethal distending toxin of *Haemophilus ducreyi* induces apoptotic death of Jurkat T cells. Infect. Immun. **67:**6394–6402.
24. **Ghosh, S., M. J. May, and E. B. Kopp.** 1998. NF-kappa B and Rel proteins: evolutionarily conserved mediators of immune responses. Annu. Rev. Immunol. **16:**225–260.
25. **Grunden, A. M., and K. T. Shanmugam.** 1997. Molybdate transport and regulation in bacteria. Arch. Microbiol. **168:**345–354.
26. **Hallstrom, T., E. Trajkovska, A. Forsgren, and K. Riesbeck.** 2006. *Haemophilus influenzae* surface fibrils contribute to serum resistance by interacting with vitronectin. J. Immunol. **177:**430–436.
27. **Hopkins, P. A., and S. Sriskandan.** 2005. Mammalian Toll-like receptors: to immunity and beyond. Clin. Exp. Immunol. **140:**395–407.
28. **Hsu, Y. M., N. Chin, C. F. Chang, and Y. F. Chang.** 2003. Cloning and characterization of the *Actinobacillus pleuropneumoniae fur* gene and its role in regulation of ApxI and AfuABC expression. DNA Seq. **14:**169–181.
29. **Izano, E. A., I. Sadovskaya, E. Vinogradov, M. H. Mulks, K. Velliyagounder, C. Ragunath, W. B. Kher, N. Ramasubbu, S. Jabbouri, M. B. Perry, and J. B. Kaplan.** 2007. Poly-N-acetylglucosamine mediates biofilm formation and antibiotic resistance in *Actinobacillus pleuropneumoniae*. Microb. Pathog. **43:**1–9.
30. **Jacobsen, I., J. Gerstenberger, A. D. Gruber, J. T. Bosse, P. R. Langford, I. Hennig-Pauka, J. Meens, and G. F. Gerlach.** 2005. Deletion of the ferric uptake regulator Fur impairs the in vitro growth and virulence of *Actinobacillus pleuropneumoniae*. Infect. Immun. **73:**3740–3744.
31. **Jacobsen, I. D., J. Meens, N. Baltes, and G. F. Gerlach.** 2005. Differential expression of non-cytoplasmic *Actinobacillus pleuropneumoniae* proteins induced by addition of bronchoalveolar lavage fluid. Vet. Microbiol. **109:**245–256.
32. **Jacques, M., J. Labrie, F. St Michael, A. D. Cox, M. A. Paradis, C. P. Dick, C. Klopfenstein, A. Broes, N. Fittipaldi, and M. Gottschalk.** 2005. Isolation of an atypical strain of *Actinobacillus pleuropneumoniae* serotype 1 with a truncated lipopolysaccharide outer core and no O-antigen. J. Clin. Microbiol. **43:**3522–3525.

33. **Jarma, E., G. Corradino, and L. B. Regassa.** 2004. Anaerobiosis, growth phase and *Actinobacillus pleuropneumoniae* RTX toxin production. Microb. Pathog. **37:**29–33.
34. **Jeannotte, M. E., M. Abul-Milh, J. D. Dubreuil, and M. Jacques.** 2003. Binding of *Actinobacillus pleuropneumoniae* to phosphatidylethanolamine. Infect. Immun. **71:**4657–4663.
35. **Jones, R. W., A. Lamont, and P. B. Garland.** 1980. The mechanism of proton translocation driven by the respiratory nitrate reductase complex of *Escherichia coli*. Biochem. J. **190:**79–94.
36. **Kachlany, S. C., P. J. Planet, R. DeSalle, D. H. Fine, and D. H. Figurski.** 2001. Genes for tight adherence of *Actinobacillus actinomycetemcomitans*: from plaque to plague to pond scum. Trends Microbiol. **9:**429–437.
37. **Kato, S., N. Sugimura, K. Nakashima, T. Nishihara, and Y. Kowashi.** 2005. *Actinobacillus actinomycetemcomitans* induces apoptosis in human monocytic THP-1 cells. J. Med. Microbiol. **54:**293–298.
38. **Kunsch, C., R. K. Lang, C. A. Rosen, and M. F. Shannon.** 1994. Synergistic transcriptional activation of the IL-8 gene by NF-kappa B p65 (RelA) and NF-IL-6. J. Immunol. **153:**153–164.
39. **Lernbecher, T., U. Muller, and T. Wirth.** 1993. Distinct NF-kappa B/Rel transcription factors are responsible for tissue-specific and inducible gene activation. Nature **365:**767–770.
40. **Lo, R. Y.** 2001. Genetic analysis of virulence factors of *Mannheimia* (*Pasteurella*) *haemolytica* A1. Vet. Microbiol. **83:**23–35.
41. **Martellini, A., P. Payment, and R. Villemur.** 2005. Use of eukaryotic mitochondrial DNA to differentiate human, bovine, porcine and ovine sources in fecally contaminated surface water. Water Res. **39:**541–548.
42. **Meyer, D. H., J. E. Lippmann, and P. M. Fives-Taylor.** 1996. Invasion of epithelial cells by *Actinobacillus actinomycetemcomitans:* a dynamic, multistep process. Infect. Immun. **64:**2988–2997.
43. **Meyer, D. H., P. K. Sreenivasan, and P. M. Fives-Taylor.** 1991. Evidence for invasion of a human oral cell line by *Actinobacillus actinomycetemcomitans*. Infect. Immun. **59:**2719–2726.
44. **Nishikori, M.** 2005. Classical and alternative NF-kB activation pathways and their roles in lymphoid malignancies. J. Clin. Exp. Hematop. **45:**15–24.
45. **Paradis, S. E., D. Dubreuil, S. Rioux, M. Gottschalk, and M. Jacques.** 1994. High-molecular-mass lipopolysaccharides are involved in *Actinobacillus pleuropneumoniae* adherence to porcine respiratory tract cells. Infect. Immun. **62:**3311–3319.
46. **Paradis, S. E., J. D. Dubreuil, M. Gottschalk, M. Archambault, and M. Jacques.** 1999. Inhibition of adherence of *Actinobacillus pleuropneumoniae* to porcine respiratory tract cells by monoclonal antibodies directed against LPS and partial characterization of the LPS receptors. Curr. Microbiol. **39:**313–0320.
47. **Peterson, J. D., L. A. Umayam, T. Dickinson, E. K. Hickey, and O. White.** 2001. The comprehensive microbial resource. Nucleic Acids Res. **29:**123–125.
48. **Ramjeet, M., V. Deslandes, F. St Michael, A. D. Cox, M. Kobisch, M. Gottschalk, and M. Jacques.** 2005. Truncation of the lipopolysaccharide outer core affects susceptibility to antimicrobial peptides and virulence of *Actinobacillus pleuropneumoniae* serotype 1. J. Biol. Chem. **280:**39104–39114.
49. **Rosan, B., J. Slots, R. J. Lamont, M. A. Listgarten, and G. M. Nelson.** 1988. *Actinobacillus actinomycetemcomitans* fimbriae. Oral Microbiol. Immunol. **3:**58–63.
50. **Saeed, A. I., V. Sharov, J. White, J. Li, W. Liang, N. Bhagabati, J. Braisted, M. Klapa, T. Currier, M. Thiagarajan, A. Sturn, M. Snuffin, A. Rezantsev, D. Popov, A. Ryltsov, E. Kostukovich, I. Borisovsky, Z. Liu, A. Vinsavich, V. Trush, and J. Quackenbush.** 2003. TM4: a free, open-source system for microarray data management and analysis. BioTechniques **34:**374–378.
51. **Schaller, A., R. Kuhn, P. Kuhnert, J. Nicolet, T. J. Anderson, J. I. MacInnes, R. P. Segers, and J. Frey.** 1999. Characterization of apxIVA, a new RTX determinant of *Actinobacillus pleuropneumoniae*. Microbiology **145:**2105–2116.
52. **Seo, S. H., O. Goloubeva, R. Webby, and R. G. Webster.** 2001. Characterization of a porcine lung epithelial cell line suitable for influenza virus studies. J. Virol. **75:**9517–9525.
53. **Sheehan, B. J., J. T. Bosse, A. J. Beddek, A. N. Rycroft, J. S. Kroll, and P. R. Langford.** 2003. Identification of *Actinobacillus pleuropneumoniae* genes important for survival during infection in its natural host. Infect. Immun. **71:**3960–3970.
54. **Sheehan, B. J., P. R. Langford, A. N. Rycroft, and J. S. Kroll.** 2000. [Cu, Zn]-Superoxide dismutase mutants of the swine pathogen *Actinobacillus pleuropneumoniae* are unattenuated in infections of the natural host. Infect. Immun. **68:**4778–4781.
55. **St Geme, J. W., III, D. Cutter, and S. J. Barenkamp.** 1996. Characterization of the genetic locus encoding *Haemophilus influenzae* type b surface fibrils. J. Bacteriol. **178:**6281–6287.
56. **Straw, B. E.** 2006. Diseases of swine, 9th ed. Blackwell Publishing, Ames, IA.
57. **Tang, G., T. Ruiz, R. Barrantes-Reynolds, and K. P. Mintz.** 2007. Molecular heterogeneity of EmaA, an oligomeric autotransporter adhesin of *Aggregatibacter* (*Actinobacillus*) *actinomycetemcomitans*. Microbiology **153:**2447–2457.
58. **Tomich, M., P. J. Planet, and D. H. Figurski.** 2007. The tad locus: postcards from the widespread colonization island. Nat. Rev. **5:**363–375.
59. **van der Rest, M. E., C. Frank, and D. Molenaar.** 2000. Functions of the membrane-associated and cytoplasmic malate dehydrogenases in the citric acid cycle of *Escherichia coli*. J. Bacteriol. **182:**6892–6899.
60. **Vanier, G., A. Szczotka, P. Friedl, S. Lacouture, M. Jacques, and M. Gottschalk.** 2006. *Haemophilus parasuis* invades porcine brain microvascular endothelial cells. Microbiology **152:**135–142.
61. **Van Overbeke, I., K. Chiers, G. Charlier, I. Vandenberghe, J. Van Beeumen, R. Ducatelle, and F. Haesebrouck.** 2002. Characterization of the in vitro adhesion of *Actinobacillus pleuropneumoniae* to swine alveolar epithelial cells. Vet. Microbiol. **88:**59–74.
62. **Wang, H., and R. P. Gunsalus.** 2003. Coordinate regulation of the *Escherichia coli* formate dehydrogenase *fdnGHI* and *fdhF* genes in response to nitrate, nitrite, and formate: roles for NarL and NarP. J. Bacteriol. **185:**5076–5085.
63. **Zhang, Y., J. M. Tennent, A. Ingham, G. Beddome, C. Prideaux, and W. P. Michalski.** 2000. Identification of type 4 fimbriae in *Actinobacillus pleuropneumoniae*. FEMS Microbiol. Lett. **189:**15–18.

Editor: V. J. DiRita